PHYSICAL REVIEW B VOLUME 23, NUMBER 9 1 MAY 1981

Interplay of structure and magnetic properties in MnSi, a concentrated spin-glass

T. M. Hayes, J. W. Allen, and J. B. Boyce
Xerox Palo Alto Research Center, Palo Alto, California 94304

J. J. Hauser
Bell Laboratories, Murray Hill, New Jersey 07974

(Received 31 October 1980)

We have performed an extended x-ray-absorption fine-structure (EXAFS) measurement of the Mn environment in amorphous (*a*-)MnSi. Whereas the Mn magnetic moments in crystalline MnSi order as a helical antiferromagnet below 29 K, *a*-MnSi is a concentrated spin-glass with a transition temperature of 22 K. The nearest neighbors of Mn in *a*-MnSi are shown to consist of five to six Si atoms at a mean distance of 2.43 ± 0.02 Å. There is no evidence for either a single close Si neighbor or a well-defined shell of Mn neighbors, such as are found in the crystal. We propose a framework within which the different magnetic behaviors of the crystalline and amorphous forms can be understood in terms of atomic order and competing magnetic interactions. We also discuss the implications of observing spin-glass behavior in concentrated as well as dilute moment systems.

I. INTRODUCTION

Crystalline (*c*-)MnSi has attracted considerable attention due to its interesting magnetic properties. Although the monosilicides of Cr, Mn, Fe, and Co are isostructural, only MnSi exhibits magnetic ordering.[1,2] Below 29 K, the magnetization curve and low effective moment of *c*-MnSi are suggestive of an itinerant weak ferromagnet, while the lack of spontaneous magnetization in zero field suggests antiferromagnetism. This apparent inconsistency was resolved by Ishikawa *et al.*[3] who showed that the magnetic moments in *c*-MnSi below 29 K, although aligned nearly parallel on a nearest-neighbor basis, actually form a helical antiferromagnet with a very long period (180 Å). MnSi can also be produced as a structurally amorphous solid by sputtering onto a substrate at or below ≈ 625 K.[4,5] This is very unlike most metallic compounds, which cannot be prepared in amorphous form by sputtering except at temperatures well below 300 K.[6] Despite a high concentration of magnetic moments, amorphous (*a*-)MnSi exhibits magnetic behavior characteristic of a dilute spin-glass—that is, a prominent cusp in the magnetic susceptibility χ at ≈ 22 K.[4,5,7]

The present study is motivated by a desire to understand the interplay between the observed differences in the magnetic properties of *c*- and *a*-MnSi and the underlying changes in atomic scale structure, and to gain further insight thereby into spin-glass phenomena in general. It builds upon the conceptual framework which was constructed in an earlier analysis of the effects of annealing on the magnetic properties of *c*-$Au_{0.95}Mn_{0.05}$, a dilute spin-glass.[8] In order to determine the structural differences between *c*- and *a*-MnSi, we undertook an extended x-ray-absorption fine-structure (EXAFS) measurement of the Mn environment in this material. We conclude that the nearest neighbors of Mn in *a*-MnSi consist of five to six Si atoms at a mean distance of 2.43 ± 0.02 Å. There is no evidence for either a single close Si neighbor or a well-defined shell of Mn neighbors, both of which are found in the crystal. We propose a framework within which the different magnetic behaviors of the crystalline and amorphous forms can be understood in terms of atomic order and competing magnetic interactions. Finally, we discuss the implications of observing spin-glass behavior in systems in which the magnetic moments are concentrated, unlike the archetypal dilute spin-glass.

II. EXPERIMENT

For the EXAFS measurements, thin films of *a*-MnSi were produced by sputtering onto thin aluminum substrates held at 370 K. Previous work had shown[4,5] that sputtered films are fully amorphous for all substrate temperatures at or below 625 K. As the substrate temperature is raised above 625 K, an increasing proportion of the film becomes microcrystalline. Films produced (or annealed) at 900 and 1300 K are crystalline with properties close to those of the bulk material. Consequently, thin films of *c*-MnSi were prepared by sputtering onto substrates held at 870 K. EXAFS spectra were obtained from these *c*-MnSi films and from films of *c*-Mn to serve as known spectra for the subsequent analysis of the

EXAFS data on *a*-MnSi. The measurements were carried out at 77 K using the EXAFS facilities on the focused line at the Stanford Synchrotron Radiation Laboratory in a conventional transmission experiment.

For all the samples, the ratio of incident to transmitted intensity was recorded as a function of photon energy from 0.9 keV below to 1.2 keV above the Mn *K* edge at 6.54 keV. The high concentration of absorbing atoms (Mn) in a weakly absorbing medium (Si) makes these samples nearly ideal for an EXAFS measurement. The resulting absorptance spectrum for *a*-MnSi is shown in Fig. 1(a). The EXAFS Δ was extracted from the raw data using procedures described in detail elsewhere[9] and expressed as a function of final-state electron momentum k. The EXAFS spectrum $k\Delta(k)$ for *a*-MnSi is shown in Fig. 1(b). Only one frequency is obvious in $k\Delta$, strong evidence for the presence of only one well-defined peak in the nearest-neighbor environment of Mn. The $k\Delta$'s extracted from each measured spectrum are Fourier transformed to r space, yielding the φ's shown in Fig. 2 for *a*-MnSi, *c*-MnSi, and *c*-Mn.

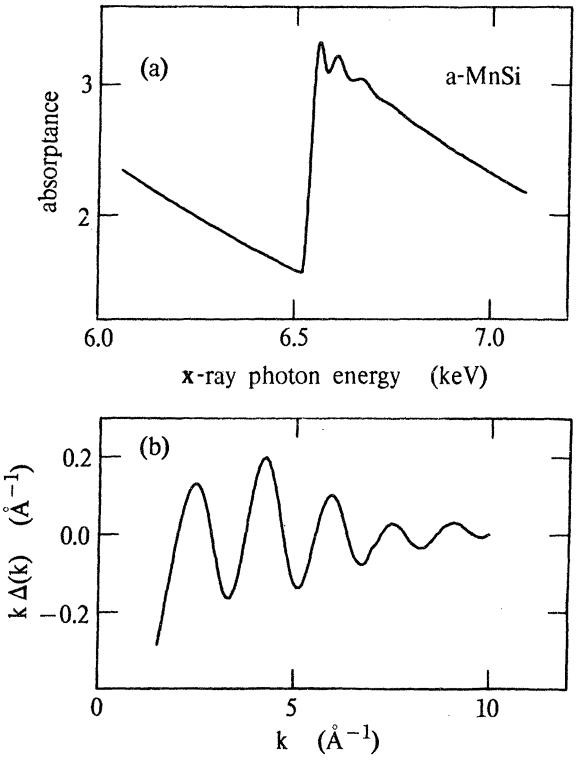

FIG. 1. (a) Absorptance of amorphous MnSi at 77 K, for a range of x-ray photon energies including the onset of the Mn *K*-shell absorption at 6.54 keV. (b) The EXAFS oscillations $k\Delta(k)$ on the Mn *K*-shell absorption in amorphous MnSi at 77 K as a function of photoelectron momentum k after removal of the background absorption and appropriate normalization.

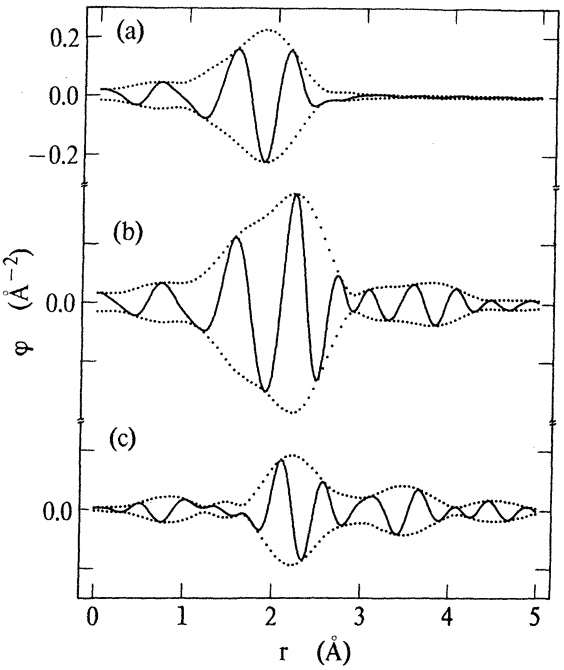

FIG. 2. Real part (solid line) and the magnitude of the Fourier transform of the EXAFS on the Mn *K*-shell absorption in three samples: (a) amorphous and (b) crystalline MnSi; (c) crystalline Mn. In each case, the k-space window is 3.15 to 8.80 Å^{-1}, broadened by 0.7 Å^{-1}. The vertical scales are identical.

The real part and magnitude of the complex φ are displayed in that figure. For *K*-shell absorption, $\varphi(r)$ can be expressed[10] as a sum of contributions from each shell of atoms surrounding the excited atom

$$\varphi(r) = \sum_{\alpha=\mathrm{Si,Mn}} \int_0^\infty \frac{dr'}{r'^2} p_\alpha(r') \xi_\alpha(r - r') \ , \qquad (1)$$

where $r > 0$ and p_α is the radial distribution function of atom species α about the excited Mn atom. p_α is defined so that $\int_0^\infty dr\, p_\alpha(r)$ equals the number of α atoms in the sample. Thus φ is a radial distribution function convolved with a peak function $\xi(r)$ (see Ref. 10 for a discussion). ξ_α is sensitive to the species α of the backscattering atom, but previous work has shown that ξ for near neighbors is relatively insensitive to changes in crystal structure, local bonding, thermal effects, etc. (e.g., see Ref. 11). Our analysis of the data is based, accordingly, on the assumption that the φ differ only because of differences in p_{Si} and p_{Mn} from sample to sample. Thus the shift or broadening of a peak in the $p(r)$ appears as a linear shift of the peak function in φ or a convolution of it with a Gaussian, respectively. φ is then a linear combination of ξ's, appropriately shifted and broadened. The details of our analysis procedure are described elsewhere.[9]

The structure of c-MnSi is $P2_13$ with four Mn and four Si atoms per unit cell (cube edge = 4.558 Å).[12] The atom positions are (u,u,u), $(\frac{1}{2}+u,\frac{1}{2}-u,-u)$, $(-u,\frac{1}{2}+u,\frac{1}{2}-u)$, and $(\frac{1}{2}-u,-u,\frac{1}{2}+u)$, where $u_{Mn}=0.138$ and $u_{Si}=0.845$. Accordingly, the nearest-neighbor environment of each Mn consists of four separate shells: one Si atom at 2.313, three Si at 2.396, three Si at 2.540, and six Mn at 2.796 Å. These four shells are all expected to contribute to the first structural feature in Fig. 2(b), between 1.2 and 2.8 Å. The nearest-neighbor environment in c-Mn is a broad distribution of Mn peaking at ≈2.68 Å, corresponding to the first structural feature in Fig. 2(c), between 1.7 and 2.8 Å. In all three parts of Fig. 2, the structure below 1 Å arises from low-frequency "noise" in the data.

Our procedure for analyzing EXAFS data[9] is based on Eq. (1), and begins with the construction of a model $p(r)$ for the unknown system. We then extract the appropriate ξ's from the φ's of the standards [for which the $p(r)$'s are known], construct a simulated φ for the unknown from the model p and these ξ's, and adjust the model p until the simulated φ agrees with the φ from the unknown according to some least-squares criterion. In this instance, however, analysis of the EXAFS data from the a-MnSi unknown must proceed differently due to the structural complexity of the c-MnSi standard. Specifically, we make an assumption about the structure of a-MnSi and then try to simulate the φ for c-MnSi on that basis. The validity of our original assumption is determined from the quality of that simulation. A similar procedure was used in Ref. 13.

Let us assume that the first peak in the radial distribution of atoms about Mn in a-MnSi arises from a single shell of Si atoms. We then try to simulate the φ for c-MnSi using a $p_{Si}(r)$ with three Gaussian peaks of known *relative* positions (e.g., r_0, $r_0+0.083$ Å, $r_0+0.227$ Å), known relative amplitudes (A_0, $3A_0$, $3A_0$), and identical widths (σ_0), as well as a $p_{Mn}(r)$ with one Gaussian peak of arbitrary position, amplitude, and width (r_{Mn}, A_{Mn}, σ_{Mn}). ξ_{Mn} was extracted from the c-Mn spectrum. The resulting six-parameter least-squares fit yielded a residual error R of 0.005 (see Ref. 9 for a definition of R). This value of R is exceptionally low. A value of $R=0.01$ to 0.02 typically corresponds to an error in φ (that is, measured φ less simulated φ) which is comparable to the noise in the EXAFS spectrum. This value of $R=0.005$ implies not only that we have simulated the data extremely well, but that the noise in the data is unusually low. The parameters deduced correspond to the first structural peak about a Mn atom in a-MnSi consisting of five to six Si atoms distributed about 2.43 ± 0.02 Å with a total Gaussian half-width of 0.11 ± 0.02 Å. The peak width includes the contributions of both static and thermal disorder. Note that 2.446 Å is the mean Mn–Si separation in c-MnSi. We find no evidence in this spectrum for a single Si atom at a shorter distance (≈2.31 Å), or for other Mn atoms. The disappearance of an EXAFS signal with increasing radial disorder has been discussed in the literature (e.g., see Ref. 10). The absence of a well-defined peak in the Mn-Mn pair correlation function in a-MnSi is especially significant. It implies that even the closest Mn-Mn pairs do not interact strongly enough to produce a well-defined distance (unlike the closest Mn-Si pairs), and is accordingly strong evidence against Mn clustering. Furthermore, it should be noted that the φ for a-MnSi is featureless beyond the first structural peak. This is commonly observed in fourfold coordinated amorphous semiconductors such as a-Si (Ref. 9) and a-Ge (Ref. 10), but is somewhat less common in highly coordinated metallic glasses.[13]

The absence of a single close Si atom and of a well-defined Mn peak from the atom distribution about a Mn atom are substantial deviations from the atomic scale order in c-MnSi. To add further substance to these conclusions of our analysis, we have used the calculated phases and backscattering amplitudes of Teo and Lee[11] to calculate the φ's expected for an excited Mn atom and both Si and Mn backscattering atoms. Adjusting the energy which corresponds to $k=0$ as they prescribe, we have been able to simulate the a-MnSi spectrum with a single Gaussian peak of Si atoms at 2.43 ± 0.02 Å and a half-width of 0.10 ± 0.02 Å ($R=0.004$). We then attempted to place as few as one Si in the region of 2.31 Å or one Mn atom anywhere between 2.40 and 2.80 Å. In every case, the quality of the simulation deteriorated. We conclude, accordingly, that there is no Mn clustering in a-MnSi, and that the Si nearest neighbors of Mn are distributed about 2.43 Å with a peak shape which is approximately Gaussian.

It is interesting to compare these results with those of an earlier EXAFS study of the Ge environment in $Pd_{80}Ge_{20}$ metallic glass.[13] Firstly, we may infer from the absence of a well-defined Mn-Mn peak in a-MnSi that only unlike atoms will be nearest neighbors in a reasonably well-annealed sample of this material. This is another manifestation of the short-range chemical order observed in the Ge environment in the earlier study. The present example is a much stronger indicator that substantial forces are involved, however, since the concentration of Mn is much higher than that of Ge in $Pd_{80}Ge_{20}$ (making chemical order that much harder to achieve). Secondly, the 5 to 6 Si atoms found about Mn is a small number compared with the 12 neighbors found[14] about Pd in $Pd_{84}Si_{16}$ and the 8 to 9 found about Ge in amorphous $Pd_{84}Ge_{20}$. This number *is* comparable, however, to the number of nearest neighbors found in the the metallic melts of Si and Ge. Such a reduced coordination number suggests the importance of wave-

function hybridization (i.e., MnSi is not a simple free-electron metal). Finally, the Mn-Si nearest-neighbor peak is relatively narrow and has a mean position significantly less than the sum of the metallic radii, which is 2.58 Å. These qualitative conclusions apply as well to amorphous $Pd_{80}Ge_{20}$,[13] and are further indicators of forces which are not free-electron-like.

III. MAGNETIC PROPERTIES OF MnSi

Before introducing our model for the interrelationship between structure and magnetic properties in MnSi, we summarize briefly the magnetic properties of this material. At high temperatures, *c*-MnSi is paramagnetic with an atomic moment measured variously at 1.4 or $2.2\mu_B$ (Refs. 15 and 2, respectively), to be contrasted with values $\approx 4\mu_B$ which are more typical of Mn in a metallic environment. The effective Mn atomic moment has presumably been reduced by interaction with Si atoms. The high-temperature χ extrapolates to a paramagnetic Curie point $\Theta \approx 30$ K.[2] As the temperature is lowered past 50 K, χ deviates from ideal Curie-Weiss behavior to lower values.[7] Finally, the Mn moments order below 29 K into an antiferromagnetic helix with a period of 180 Å.[3] In this structure, the Mn-Mn nearest-neighbor moments are aligned nearly parallel, but the net moment vanishes in zero field due to the long period helix. The magnetic susceptibility χ saturates as one might expect.[16] The effective moment in this ordered structure has been determined to be $0.4\mu_B$.[15,17]

At high temperatures, *a*-MnSi is also paramagnetic, with an effective moment of $2.6\mu_B$.[5,7] Its high-temperature χ extrapolates to a Θ which ranges from 30 K for a substrate temperature during sputtering T_s of 77 K (Ref. 7) to 65 K for $T_s = 350$ (Ref. 5). As the temperature is lowered, χ falls below ideal Curie-Weiss behavior for temperatures below 80 K for $T_s = 77$ K (Ref. 7) [or below 100 K for $T_s = 350$ K (Ref. 5)]. χ shows only a slight feature near the ordering temperature for the crystal (29 K). Instead, at a temperature ≈ 22 K, χ exhibits the sort of cusp which is the hallmark of a spin-glass.[4,5,7,18]

A rather detailed earlier study[5] of *a*-MnSi yielded two further observations which are particularly interesting in this context. As the substrate temperature during deposition is increased from 77 to 320 to 625 K, the magnitude of the cusp in the susceptibility increases from 0.4 to 1.6 to 4.4×10^{-3} emu/g, respectively. This was attributed to increased Mn clustering with increasing substrate temperature, which we now hold to be inconsistent with our EXAFS measurement. Additionally, increasing the Mn concentration to $Mn_{0.6}Si_{0.4}$ and $Mn_{0.7}Si_{0.3}$ (with a substrate temperature of 370 K) decreased the magnitude of the cusp in χ to 1.2×10^{-3} and 0.2×10^{-3} emu/g.

IV. MODEL FOR THE RELATIONSHIP BETWEEN STRUCTURE AND MAGNETIC PROPERTIES

In an earlier paper,[8] we reported a measurement of the Mn environment as a function of annealing in *c*-$Au_{0.95}Mn_{0.05}$, a dilute spin-glass, and discussed at some length the interrelationship between the atomic scale structure and the magnetic properties. The following model incorporates the added features of concentrated moments and amorphous structure in ways which are fully consistent with the concept of a spin-glass as discussed in that work. From the structure and magnetic properties of *c*-MnSi, we identify the dominant Mn-Mn pairwise interactions in this environment, both electronic and magnetic. The different low-temperature magnetic properties of the crystalline and amorphous forms of MnSi are shown to flow naturally from these interactions, given the differences in long-range atomic order.

As noted above, the Mn nearest-neighbor environment in *c*-MnSi includes one Si atom at 2.313 Å, three Si atoms each at 2.396 and 2.540 Å, and six Mn atoms at 2.796 Å. The metallic radius of Mn is 1.261 Å, while the covalent and metallic radii of Si are 1.11 and 1.316 Å, respectively. Thus the Mn–Si separations range about those expected for covalent Si (2.371 Å) and are substantially less than that expected for metallic Si (2.577 Å). From both the mean distance and the spread in distances, we infer that the Mn-Si interaction is direct, and intermediate between metallic and covalent. In contrast, the Mn–Mn distance is substantially larger than twice its metallic radius (2.522 Å) and also large compared with the normal range of radii in crystalline Mn (which has few nearest neighbors beyond 2.68 Å). Consequently, we infer that the Mn interaction is indirect, via intermediary Si atoms. Indeed, as we noted earlier, MnSi is not a simple free-electron metal. There is substantial evidence that the electronic structure is determined primarily by extensive hybridization between the metalloid (Si) *p* states and the metal *d* states, both for MnSi in particular[19] and for transition-metal–metalloid compounds and alloys in general.[20] Turning to *a*-MnSi, we expect that these conclusions about the interatomic interactions in *c*-MnSi will be equally valid. The spread of nearest-neighbor Mn–Si distances is expected to collapse into a single broad distribution once the constraints of long-range order are removed. This is consistent with the deduction from the EXAFS data of a single broad peak of Si about Mn, with a mean separation of 2.43 Å. If the Mn-Mn interaction in MnSi is indirect as we believe, then we expect that the Mn-Mn nearest-neighbor peak in *a*-MnSi would be substantially broadened without the constraints of long-range order. This is reflected in the absence of a Mn-Mn contribution from the EXAFS spectrum.

In *c*- and *a*-MnSi at high temperatures, χ shows

ideal Curie-Weiss behavior with effective moments in the range of 1.4 to 2.6μ_B. The measured paramagnetic Curie point Θ ranges from 30 to 65 K. We infer from this positive value of Θ that the *dominant* interaction in each case is ferromagnetic. As the temperature is lowered past approximately 2Θ, both phases show deviations from the ideal Curie-Weiss behavior in the direction of smaller values of χ. The direction of the deviations suggests the increasing importance of some antiferromagnetic interaction in determining the magnetic properties.

Ultimately, at 29 K, the long-range order in the crystal allows the establishment of a long-period magnetic superlattice to ameliorate the growing conflict between the ferromagnetic and antiferromagnetic interactions. Although the magnetic moments are aligned perpendicular to a $\langle 111 \rangle$ direction and nearly parallel to near-neighbor moments, the moment direction rotates once about that axis every $\approx$180 Å. There have been several discussions of the origin of this unusual magnetic structure. Ishikawa *et al.*[3] analyzed the Heisenberg model for the case of the MnSi crystal structure and established the conditions which must be met by the exchange interactions in order for the long period helix to exist. Assuming that the closest-neighbor moment-moment interaction (that between Mn moments 2.80 Å apart) is antiferromagnetic, they determined that these conditions could not be met and concluded accordingly that the Heisenberg model was probably not applicable. Subsequently, Moriya[21] and Makoshi[22] attributed the helix to the occurrence, at the helix wave vector, of a maximum in the magnetic susceptibility of the noninteracting electron system. Band-structure calculations[19] for MnSi do not support this picture, however, leading Nakanishi *et al.*[23] to propose that the helix results from a free-energy term involving the spin-orbit interaction. Despite these efforts, no detailed microscopic model has predicted successfully the observed magnetic ordering.

It appears to us, however, that the Heisenberg model suffices to demonstrate the necessity of competing exchange interactions. Motivated by evidence for a dominant ferromagnetic interaction, which is contrary to the assumption made by Ishikawa *et al.*,[3] we have reexamined the conditions given by them for helix formation within the Heisenberg model. These conditions are satisfied easily if the closest-neighbor exchange interaction J_1 is ferromagnetic (at $r_{\mathrm{Mn-Mn}} = 2.80$ Å) and the next-closest-neighbor interactions J_2 are weaker and antiferromagnetic (at $r_{\mathrm{Mn-Mn}} = 4.15$, 4.38, and 4.56 Å). A similar model was used recently to describe magnetic torque measurements in MnSi.[24] The values $J_1 = 0.55$ and $J_2 = -0.08$ meV lead to the experimental value[3] of $q = 0.035$ Å^{-1} for the wave vector which minimizes the magnetic energy, and also to the experimental paramagnetic Curie point $\Theta = 30$ K, assuming a spin of unity. It should be possible to impose an additional condition on the J values using a molecular field formula for the Néel temperature T_N (see Ref. 25). We are not satisfied with the results of this procedure, however, since the simplest extension of our equations predicts that $|\Theta - T_N|$ must be less than 10^{-6} K for such a small value of q. If experiment demands a larger value of $|\Theta - T_N|$ consistent with $q \approx 0.035$ Å^{-1} (which it does not at the moment), a more complex set of equations would be required. Nonetheless, we conclude that the competition between a close-neighbor ferromagnetic interaction and a weaker further-neighbor antiferromagnetic interaction underlies the helical antiferromagnetism of c-MnSi as well as the deviations in χ from ideal Curie-Weiss behavior in both c- and a-MnSi.

Given the same competing pairwise magnetic interactions, the moments in the amorphous sample cannot order as in the crystal, due to the lack of the appropriate long-range atomic order. There is, however, a slight feature in χ observable for most amorphous samples in the region of 30 to 35 K. For a-MnSi, the growing conflict between ferromagnetic and antiferromagnetic interactions is resolved at $\approx$22 K by the locking in of a disordered array of moments—a spin-glass transition.

In both the crystalline and amorphous forms of MnSi, the magnetic behavior can be understood only in terms of a conflict between ferromagnetic and antiferromagnetic interactions among the Mn moments. Since the temperatures at which changes occur in the magnetic properties vary only moderately from c- to a-MnSi, we must conclude that the magnitudes of these interactions are relatively insensitive to the structural differences. In other words, the fundamental interactions between the Mn moments are relatively insensitive to the long-range chemical order, and depend primarily upon certain elements of short-range chemical order which are preserved in both solid phases. This is easier to understand if we believe that the principal magnetic interaction among the Mn atoms is through intermediary Si atoms, in analogy with our earlier conclusion regarding the chemical interaction among Mn atoms. While the Mn-Si arrangement does change in some ways between the crystal and the amorphous form, the mean position and the number (to a lesser extent) of the Si atoms are similar in the two phases. Apart from the magnetic ordering, those modest differences in magnetic properties which do exist between the two phases are probably due to those slight changes in the number of Si neighbors and in the Mn-Si-Mn "bond angles" which occur in the amorphous form. The essential competing ferromagnetic and antiferromagnetic interactions appear, however, to be largely unchanged between the crystalline and amorphous forms. It is the response of the solid to that competition which depends necessarily and strikingly upon

the presence or absence of long-range atomic order.

It is possible to force changes in these interactions, however, and we believe that this explains two of the observations for the amorphous system. If we force the occurrence of Mn-Mn nearest neighbors, then the antiferromagnetic interaction which is observed in elemental Mn should reduce the effective moment and lower the susceptibility noticeably. One way to force the occurrence of Mn-Mn nearest-neighbor pairs is to increase the concentration of Mn in the amorphous state. That indeed led to a strong reduction in χ as noted earlier.[5] Additionally, one could try to freeze in this short-range chemical disorder during the sputtering process. This should be easier than in the case of a dilute system, because it is more difficult to have only unlike nearest-neighbor pairs in a 50-50 system. Indeed, it would appear that Mn-Mn pairs do occur in *a*-MnSi sputtered at 77 K, since the magnitude of χ increases substantially with the annealing of that sample at 300 K. Further increases in deposition temperature will result in subtle annealing effects in the amorphous solid which might also increase the effective moment, as pointed out in our earlier treatment of *c*-$Au_{0.95}Mn_{0.05}$.[8] In that study, it was argued that the increase in the prominence of the cusp in χ with annealing resulted from subtle changes in the number of Mn moments in second- and third-neighbor positions to other Mn ($r_{Mn-Mn}=4.07$ and 4.99 Å), in strict analogy with the magnetic behavior of Au-Mn compounds.

There is one observation which does not fit into the model as stated above. Hauser *et al.*[5] reported that the position and magnitude of the cusp in the χ of a presumably microcrystalline sample sputtered at 675 K are essentially the same as those of amorphous samples sputtered below 625 K. In contrast, the simplest extension of our model to a microcrystalline form of MnSi would lead to the anticipation of ferromagnetic behavior. A likely explanation for this apparent inconsistency is that that sample is in fact largely amorphous. If that sample is truly microcrystalline, the model described above would require either a sophisticated extension to cover the microcrystalline state of MnSi, or some fundamental revision.

How do we understand spin-glass phenomena in a system with a high concentration of moments? It appears as though the only problem posed by a concentrated system is the added difficulty of introducing disorder into the dominant magnetic interactions. In an earlier treatment of the annealing dependence of spin-glass behavior in a dilute crystalline system, $Au_{0.95}Mn_{0.05}$, we noted that the forces which order the Mn positions on the lattice are relatively weak second- or third-neighbor chemical forces. Consequently, Mn atoms are not ordered in the spin-glass sample. In fact, the spin-glass behavior would disappear if an ordered array of Mn moments were to be produced in that system (barring the occurrence of a truly "frustrated" arrangement). In a concentrated system, on the other hand, a great deal of moment order can be established by strong nearest-neighbor chemical forces. Thus, disorder of the magnetic interactions is difficult to achieve *unless* the crystalline order is eliminated, as is the case in *a*-MnSi. In other words, in addition to an adequate amount of antiferromagnetic coupling, a spin-glass requires sufficient disorder among the dominant magnetic interactions. These elements are present in *c*-$Au_{0.95}Mn_{0.05}$ and *a*-MnSi (where the Mn positions are in fact disordered), but not in *c*-MnSi. In the last system, the crystalline order allows other solutions to energy minimization given the competing interactions—that is, the long period helical antiferromagnet.

V. SUMMARY

We have performed an extended x-ray-absorption fine-structure (EXAFS) measurement of the Mn environment in *a*-MnSi. The nearest neighbors of Mn in *a*-MnSi consist of five to six Si atoms at a mean distance of 2.43 ± 0.02 Å. There is no evidence for either a single close Si neighbor or a well-defined shell of Mn neighbors, such as are found in the crystal. We propose a framework within which the different magnetic behaviors of the crystalline and amorphous forms can be understood in terms of atomic order and competing magnetic interactions. Specifically, we conclude that the magnetic properties of MnSi are determined by competing ferromagnetic and antiferromagnetic interactions which differ only slightly between *c*- and *a*-MnSi. The striking differences in magnetic properties arise from the fact that the two forms have different routes available for the relaxation of this competition. Finally, we conclude that the observation of spin-glass behavior in concentrated moment systems is unusual only to the extent that the requisite disorder in the magnetic interactions is more difficult to achieve.

ACKNOWLEDGMENTS

Some of the materials incorporated in this work were developed at the Stanford Synchrotron Radiation Laboratory with the finanical support of the National Science Foundation (under Contract No. DMR 77-27489), in cooperation with the Department of Energy.

[1]D. Shinoda and S. Asanabe, J. Phys. Soc. Jpn. 21, 555 (1966).
[2]J. H. Wernick, G. K. Wertheim, and R. C. Sherwood, Mater. Res. Bull. 7, 1431 (1972).
[3]Y. Ishikawa, K. Tajima, D. Bloch, and M. Roth, Solid State Commun. 19, 525 (1976).
[4]J. J. Hauser, Solid State Commun. 30, 201 (1979).
[5]J. J. Hauser, F. S. L. Hsu, G. W. Kammlott, and J. V. Waszczak, Phys. Rev. B 20, 3391 (1979).
[6]G. S. Cargill, III, in *Solid State Physics*, edited by H. Ehrenreich, F. Seitz, and D. Turnbull (Academic, New York, 1976), Vol. 30, p. 227.
[7]R. W. Cochrane, J. O. Strom-Olsen, and J. P. Rebouillat, J. Appl. Phys. 50, 7348 (1979).
[8]T. M. Hayes, J. W. Allen, J. B. Boyce, and J. J. Hauser, Phys. Rev. B 22, 4503 (1980).
[9]T. M. Hayes, J. Non-Cryst. Solids 31, 57 (1978).
[10]T. M. Hayes, P. N. Sen, and S. H. Hunter, J. Phys. C 9, 4357 (1976).
[11]B.-K. Teo and P. A. Lee, J. Am. Chem. Soc. 101, 2815 (1979).
[12]Y. Ishikawa, G. Shirane, J. Tarvin, and M. Kohgi, Phys. Rev. B 16, 4956 (1977).
[13]T. M. Hayes, J. W. Allen, J. Tauc, B. C. Giessen, and J. J. Hauser, Phys. Rev. Lett. 40, 1282 (1978).
[14]J. F. Sadoc and J. Dixmier, in *The Structure of Non-Crystalline Materials*, edited by P. H. Gaskell (Taylor and Francis, London, 1977), p. 85.
[15]H. J. Williams, J. H. Wernick, R. C. Sherwood, and G. K. Wertheim, J. Appl. Phys. 37, 1256 (1966).
[16]C. N. Guy, Solid State Commun. 25, 169 (1978).
[17]D. Bloch, J. Voiron, V. Jaccarino, and J. H. Wernick, Phys. Lett. 51A, 259 (1975).
[18]See, for a general discussion of spin-glasses, a review by J. A. Mydosh, J. Magn. Magn. Mater. 7, 237 (1978).
[19]O. Nakanishi, A. Yanase, and A. Hasegawa, J. Magn. Magn. Mater. 15–18, 879 (1980).
[20]J. W. Allen, A. C. Wright, and G. A. N. Connell, J. Non-Cryst. Solids (in press).
[21]T. Moriya, Solid State Commun. 20, 291 (1976).
[22]K. Makoshi and T. Moriya, J. Phys. Soc. Jpn. 44, 80 (1978).
[23]O. Nakanishi, A. Yanase, A. Hasegawa, and M. Kataoka, Solid State Commun. (in press).
[24]C. N. Guy and J. O. Strom-Olsen, J. Appl. Phys. 50, 1667 (1979).
[25]J. S. Smart, *Effective Field Theories of Magnetism* (Saunders, Philadelphia, 1966), p. 104.